Clays and Clay Minerals, Vol. 59, No. 1, 42–57, 2011.

THE EFFECT OF SURFACE CHARGE AND WETTABILITY ON H_2O SELF DIFFUSION IN COMPACTED CLAYS

BIRGIT SCHAMPERA[1,*] AND STEFAN DULTZ[1,2]

[1] Institute of Soil Science, Leibniz University Hannover, Herrenhäuser Str. 2, D-30419, Hannover, Germany
[2] ZFM – Center for Solid State Chemistry and New Materials, Leibniz University Hannover, Germany

Abstract—Organo-clays are of interest in the modification of anion transport properties in engineered barriers. In the present study, surface charge and wettability were assessed for tracking changes in the effective diffusion coefficient (D_{eff}) by the formation or suppression of bound H_2O layers on the external surfaces of clays. Bentonite samples modified with three different organic cations in amounts of 0 to 400% of the cation exchange capacity were used. Diffusive transport was determined in $H_2O \rightarrow D_2O$ exchange experiments in a newly constructed cell adapted to the attenuated total reflectance (ATR) accessory of a Fourier-transform infrared (FTIR) spectrometer at two different dry bulk densities and various degrees of water saturation.

All organo-clay combinations showed changes in surface charge after the addition of organic cations, from a negative value of 99 $mmol_c/kg$ for the original bentonite to a maximum positive value of 230.5 $mmol_c/kg$ for hexadecylpyridinium (HDPy)-montmorillonite. The positive charge resulted from adsorption of the organic cation in excess of the CEC. Hydrophobic surface properties with contact angles >90º were obtained for HDPy-montmorillonite samples with monolayers of organic cations on the external surfaces only. Here, where hydrophobicity suppressed the formation of bound H_2O layers, the largest D_{eff} of 2.7×10^{-10} m^2/s was observed in the high dry bulk density range (1.0–1.5 g/cm^3) under water-saturated conditions. In the low dry bulk density range (0.6–0.9 g/cm^3) this effect was weakened significantly because, with increasing pore size, the effect of bound H_2O layers was reduced. In the high dry bulk density range at partial water saturation (40%), diffusive transport was hindered by the small water volume. Previous work found that, in the high dry bulk density range and water-saturated state, D_{eff} was 2.4×10^{-11} m^2/s for the original bentonite. D_{eff} for all hydrophilic organo-clay samples was $\leqslant 2.1 \times 10^{-11}$ m^2/s, somewhat less than for the hydrophobic sample. In hydrophilic organo-clay samples, retardation factors that retard the value for D_{eff}, up to a magnitude of 0.5, include an increase in dry bulk density and a decrease in water saturation. In the water-saturated state at high dry bulk densities, hydrophobic surface properties suppressing the formation of bound H_2O layers can increase D_{eff} by one order of magnitude.

Key Words—Bentonite, Bound H_2O, Diffusive Transport, Organo-clays, Surface Charge, Wettability.

INTRODUCTION

In water-saturated pores of clays, both free water and bound H_2O co-exist in layers at the surfaces of these charged minerals. The solid surface modifies the structure of water in the adsorbed layers significantly. Compared to bulk water in the liquid, the mobility of these adsorbed molecules is reduced by more than one order of magnitude due to a distorted hydrogen-bond network, which significantly differs from that of bulk water (Michot *et al.*, 2002). Bound H_2O layers have a thickness of several nanometers (Ichikawa *et al.*, 2001). The presence of bound H_2O layers is important for transport processes, as self diffusion of water is fastest in bulk water and is slowed in bound H_2O (Marry *et al.*, 2008). Due to low self-diffusivity in bound H_2O caused by temporary binding, those bound layers increase the apparent volume of platelets and act as obstacles to diffusion (Duval *et al.*, 2001). This obstruction effect of less mobile water consequently decreases the H_2O self-diffusion coefficient (Nakashima, 2003).

The uncharged phyllosilicates, talc and pyrophyllite, have hydrophobic surfaces which suppress the formation of bound H_2O layers. In permanently charged phyllosilicates, such as smectites, illites, and chorites, bound H_2O layers are present on the surface. Their thickness depends on layer charge, ionic strength, and type of adsorbed cation. By Monte Carlo simulations, Marry *et al.* (2008) calculated two to three bound H_2O layers for montmorillonite, the number being more strongly influenced by charge density than by the type of counter ion (Johnston and Tombacz, 2002). The large hydration energy of small multivalent cations strongly polarizes H_2O molecules whereas large monovalent cations are weakly hydrated. Despite these different ionic properties, diffusive transport is only weakly influenced by the kind of inorganic cation embedded within the bound H_2O layer (Ichikawa *et al.*, 1999). As layer charge increases, the thickness of the bound H_2O layer also increases, revealing

* E-mail address of corresponding author:
schampera@ifbk.uni-hannover.de
DOI: 10.1346/CCMN.2011.0590107

that charge density is the more important factor for obstructing diffusion (Nakashima and Mitsumori, 2005). From determinations on different 2:1 layer silicates, tetrahedral substitution was concluded to have a distinct effect on the clay-water interaction with respect to the stabilization energy (Chatterjee *et al.*, 1997). In addition, the type of diffusing species affects transport. Repulsive electrostatic forces between the negatively charged clay surface and anions result in a smaller pore volume available for anion transport (Van Loon *et al.*, 2007). With increasing ionic strength of the solution the anion exclusion effect is diminished. An increase in dry bulk density to >1.4 g/cm^3 enhances water release from the interlayer. As a consequence, in the dry state the amount of water adjacent to the surface is increased, which in turn decreases the pore space and increases the activation energy of diffusion, *e.g.* of chloride ions (Kozaki *et al.*, 2001).

Besides the properties of the interface, diffusive transport in clays is governed by the accessible pore volume and pore geometry. The geometrical properties of the particles control the pore-network geometry by affecting the size, orientation, shape, and connectivity of pores (Bourg *et al.*, 2006) and, thereby, the tortuosity and diffusive transport. With decreasing pore size the effect of bound H_2O layers on diffusive transport increases. In compacted bentonite, two typical pore throat radii with maxima at 0.02 and 2 μm, measured in the dry state, are observed. The first group corresponds to inter-particle voids between the particles inside the aggregates and the second to inter-aggregate pores (Delage *et al.*, 2006). With increasing dry bulk density, the share of the small inter-particle pores increases, in addition to an overall shift to smaller pore sizes (Hicher *et al.*, 2000). Therefore, at high dry bulk density in particular, marked effects of bound H_2O layers on diffusion transport can be assumed.

The main function of compacted clays in engineered barriers is the reduction of advective transport through the liner and the adsorption of contaminants. As the sorption capacity of bentonites for anionic and hydrophobic pollutants is small, the use of organically modified clays with a large adsorption capacity for anions (Li and Bowman, 1998) and hydrophobic organic compounds (Rytwo *et al.*, 2007) is of interest. In addition, organo-clays have the capability to sorb anions, cations, and uncharged organic contaminants simultaneously (Bors *et al.*, 1997; Oyanedel-Craver *et al.*, 2007; Guegan *et al.*, 2009). The success of such an approach in an engineering sense depends heavily on the selectivity of the clay for exchangeable organic cations over the major cations of the groundwater. The extent of the adsorption of inorganic cations and anions, as well as the reversibility of binding, is affected by the chemical composition of the equilibrium solution (Bors *et al.*, 2000).

Changes in clay-surface properties due to the modification with organic cations such as charge reversal (Imai *et al.*, 2003) and hydrophobicity (Rytwo *et al.*, 2007) make organo-clays an interesting subject for studying the effect of different surface properties on diffusive transport. Less is known about the effect of organo-clays in clay liners on the safety of the barrier. Clay liners with up to 20% organo-bentonite (BTEA-(benzyltriethylammonium)- or HDTMA-(hexadecyltrimethylammonium)-bentonite) amendment have similar effective diffusion coefficients (D_{eff}) for tritium as the original bentonite, whereas the hydraulic conductivity of the organo-bentonite amendment by itself was much greater (Lorenzetti *et al.*, 2005), which could cause a problem for barrier performance.

In the present study, the influence of surface charge (SC) and wettability of the clay on the formation of bound H_2O layers was investigated. This was an extension of an earlier study by Schampera and Dultz (2009) in which HDPy-montmorillonite was compared with natural montmorillonite. Here, three monovalent organic cations with very different structures were chosen and applied in the concentration range from 0 to 400% of the cation exchange capacity (0−400% CEC) in 16 steps in order to obtain a large degree of variability in the surface properties. Diffusion experiments were carried out with D_2O, which is a neutral, non-reactive, and conservative tracer. The behavior of D_2O during diffusion transport was comparable to liquid water containing monovalent, inorganic cations and anions (Li and Gregory, 1974).

Because the determination of diffusion transport in cells, even at the laboratory scale, is time consuming, a time-saving *in situ* technique using attenuated total reflectance-Fourier transform infrared (ATR-FTIR) spectroscopy, introduced by Fielderson and Barbari (1993), was used. The method provides data for significant factors of diffusion transport and additional information on the interactions at the molecular level. In the FTIR spectra, D_2O is clearly detectable in the presence of H_2O by the O−D stretching vibration. The increasing H−D−O bending vibration at 1450 cm^{-1} indicates the exchange of isotopes between the water molecules. The D_{eff} for $H_2O \rightarrow D_2O$ exchange experiments on D_2O-saturated samples reflects the effective diffusivity of water molecules and protons, including the tortuosity factor and porosity. The D_{eff} values determined are discussed in light of surface properties at different degrees of organic cation uptake, the effect of water saturation, and dry bulk density. The study of diffusive transport of H_2O in organo-clays is of particular importance when the use of such clays in engineered barriers is considered.

MATERIALS AND METHODS

Preparation of organo-montmorillonites

A commercial Wyoming bentonite (MX-80) containing 75% montmorillonite was obtained from AMCOL

Specialty Minerals (Cheshire, England). The CEC determined by the Ag-thiourea method (Van Reeuwijk, 1993) was 0.86 $mol_c\ kg^{-1}$. Na is the most common exchangeable cation, with 95% of the exchange sites saturated with Na and the remainder with Ca. On the basis of the C content (Vario EL, Elementar, Germany), 1.6 wt.% $CaCO_3$ was determined to be present in the bentonite.

The bentonite was modified with three different monovalent organic cations. Hexadecylpyridinium-chloride (HDPy) and tetraphenylphosphoniumchloride (TPP) were purchased from Fluka AG (Hamburg, Germany) and benzethoniumchloride (BE) from Sigma-Aldrich Chemie, GmbH (Hamburg, Germany). HDPy is a long alkyl-chain nitrogen cation with a pyridinium ring (Figure 1). Due to the positive charge of N, the ring is hydrophilic while the alkyl chain is hydrophobic. For BE, the positively charged nitrogen is located more in the middle of the cation between two aromatic rings. The structure of BE is tortuous and cell constants of single $BECl{\cdot}H_2O$ crystals have large standard deviations due to highly fragile properties (Tanaka and Hirayama, 2008). For TPP, phosphorus is the carrier of the positive charge, tetrahedrally coordinated by four phenyl rings. Short-chain organic phosphonium salts adsorbed to clays are known to possess a greater thermal stability than that of ammonium salts (Imai *et al.*, 2003).

Organo-clays were prepared by adding solutions of organic cations to the clay suspensions (100 mg of bentonite in 10 mL of solution) in quantities of the organic cation corresponding to 2, 10, 20, 40, 50, 60, 70, 80, 90, 100, 120, 140, 150, 200, 300, and 400% CEC and shaking for 20 h at room temperature. These were the amounts applied, which in some cases differed from the amounts actually taken up or adsorbed by the clay. To remove excess salts, samples were then washed with deionized water on a 0.45 μm cellulose acetate filter and freeze dried. The amount of organic cation adsorbed was calculated from the C content of the organo-clay, determined using a CNS analyzer (Vario EL, Elementar, Germany). Examples of sample notation are HDPy-37 or HDPy-71, indicating the amount of organic cation adsorbed in % of the CEC. To determine the basal spacings, samples were dispersed in deionized water, sedimented onto glass slides, air dried, and finally measured with X-ray diffraction (XRD) using a Philips PW1390 instrument (Eindhoven, The Netherlands) equipped with Cu$K\alpha$ radiation.

Surface charge and wettability

The SC was quantified by generating a streaming potential and titration of charge-compensating polyelectrolytes using the cell of a particle charge detector (PCD 03, Mütek, Germany). The basic principle of the measurement is an electro-kinetic effect in the current (Hunter, 1993; Böckenhoff and Fischer, 2001). The end point of the titration was defined at zero potential. For negative and positive SC, the cationic polyelectrolyte poly-DADMAC (poly-diallyldimethylammoniumchloride) and the anionic polyelectrolyte PES-Na (sodium-polyethylenesulfonate) were used, respectively. The PCD technique is a well established method for studying SC properties of organo-clays (Rytwo *et al.*, 2006; An and Dultz, 2007). For each titration, 10 mg of sample was suspended in 10 mL of deionized water. After dispersion the suspension was transferred into the titration cell. Each measurement was performed at least three times. The pH of the suspensions was weakly alkaline (pH 8.3−10.1) which was due to the presence of some carbonate in the bentonite.

The wettability was determined by the Wilhelmy plate method (Woche *et al.*, 2005) using a dynamic contact-angle tensiometer with a resolution of 10^{-5} g (DCAT 11, Dataphysics, Filderstadt, Germany). To determine the contact angle (Θ), a thin layer of the sample was sprinkled and pressed onto a glass slide (28 mm × 48 mm) covered on all sides with double-sided adhesive tape and then immersed in deionized water on a

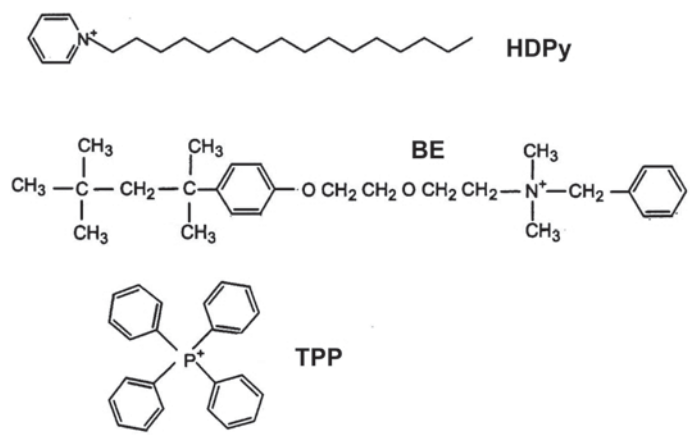

Figure 1. Structures of hexadecylpyridinium (HDPy), benzethonium (BE), and tetraphenylphosphonium (TPP).

balance. Θ was then determined by the following procedure. According to Bachmann *et al.* (2003) the dynamic contact angle, Θ, is calculated by:

$$\cos \Theta = F_w/(\sigma_{lv} l_w) \quad (1)$$

where cos Θ is the cosine of the contact angle; F_w, the wetting force (N); σ_{lv}, the surface tension of the liquid (Nm^{-1}); and l_w, the wetted length (m) of the immersed sample. The balance was tared before the measurement, so that only the buoyancy and the wetting forces acting on the sample were measured. After buoyancy-force correction by linear regression to zero immersion depth, the wetting force was calculated by the interception point. The data obtained refer to the advancing contact angle, Θ. Each sample was measured at least three times. The surface tension of the deionized water was measured before and after each Θ determination to ensure that no components of the sample (*e.g.* organic cations) dissolved during the immersion process. Here a Pt-Ir-Wilhelmy plate with known wetted length and cos Θ = 1 was used.

Diffusion experiments

To determine the D_{eff} of H_2O in the samples, two different degrees of water saturation and ranges of dry bulk density were adjusted. Samples were exchanged with organic cations comprising 0, 40, 80, 120, 200, and 400% CEC. The experiments were run in a diffusion cell (Figure 2) which was attached to a single-reflection ATR accessory (MIRacle, Pike, Madison, Wisconsin, USA) of a FTIR spectrometer (TENSOR 27, Bruker, Bremen, Germany). The diffusion cell allows the determination of D_{eff} in clays at different dry bulk densities and degrees of water saturation, typically in a short time period of 20 h (Schampera and Dultz, 2009). In the sample chamber of the cell with an inner diameter of 2.5 mm, each 7.00 mg sample was compacted to heights of 0.7 or 1.0 mm resulting in two different dry bulk density ranges of 0.6−0.9 and 1.0−1.5 g/cm^3, respectively. The dry bulk density was calculated from the height, the diameter, and the weight of the sample after drying at 105ºC. The solid density was estimated by the structural formulae of montmorillonite, the uptake of organic cations, and the basal spacings, the latter indicating the arrangement of the organic cations in the interlayer space.

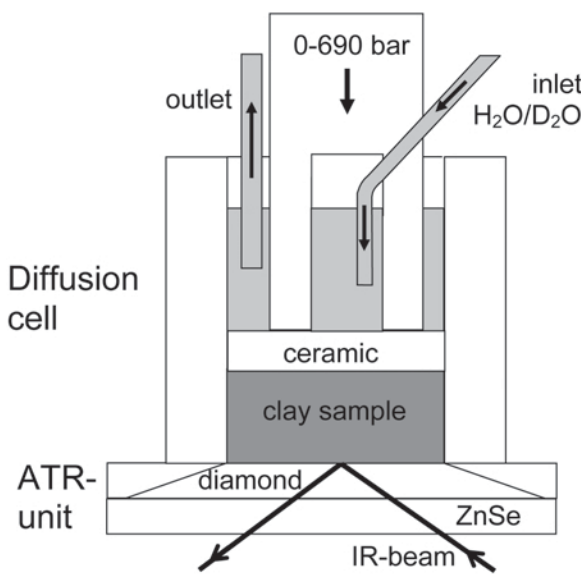

Figure 2. Illustration of the diffusion cell attached to the ATR unit of the FTIR spectrometer.

The observed variability within one dry bulk density range depends on the amount and type of organic cation adsorbed. In addition, the adjustment of sample height with the high-pressure clamp attached to the ATR unit could only be in discrete increments, which limited exact adjustment. Thus, differences in microstructure, *e.g.* for organo-clay samples which are near the point of zero charge (PZC), forming a voluminous arrangement of clay platelets (Schampera and Dultz, 2009), and some loss of sample during transfer in the sample chamber may contribute to the variability.

The pre-compacted samples were removed from the ATR cell in the Teflon cylinder and saturated with D_2O in a vacuum desiccator. The Teflon cylinder and the sample were covered with D_2O and evacuated to <10 mbar. Therefore, D_2O was pressed into the pores by applied air pressure. Afterward the clay platelet was placed in the diffusion cell and the targeted height was obtained again.

For measurements under partial water saturation, samples were placed in the Teflon cylinder, covered with a ceramic plate, and compacted to the defined height. A permanent reservoir of D_2O on top of the ceramic plate was ensured by means of a peristaltic pump. Partial water saturation was attained by advective transport of D_2O into the sample. Within 1−5 min of contact with D_2O, the O−D stretching vibration at 2480 cm^{-1} of the FTIR spectra became visible, indicating fast advection of D_2O into the samples. The absorbance of the O−D stretching vibration was stable, typically after 20 min, indicating that equilibrium conditions were reached. The average degree of water saturation was calculated from the solid density of the respective organo-clay, the volume of the clay platelets, sample-weight directly after the experiment, and after drying at 105ºC for 24 h. It was typically at 40%.

Before starting the $H_2O \rightarrow D_2O$ diffusion experiment, a spectrum of the D_2O-loaded sample was measured as a background spectrum. The recording of the spectra was started (at zero time) and, at the same time, the addition of H_2O by means of a peristaltic pump was commenced. The progress of the diffusion of H_2O was monitored by the increase in the absorbance of the O−H stretching vibration at 3380 cm^{-1}. Spectra were recorded auto-

matically in time intervals from 0.5 to 10 min until the absorbance of the O−H stretching vibration became constant, typically after 20 h. The results from this in-diffusion experiment depended on the pore-space volume and on the amount of pore water.

Modeling of diffusion data

The D_{eff} was calculated according to Fielderson and Barbari (1993) using the linear regression from a plot of $\ln(1-A_t/A_\infty)$ *vs.* time (equations 2, 3). Gradient m, obtained by linear regression, was used to calculate D_{eff} (equation 4).

$$\ln\left(1-\frac{A_t}{A_\infty}\right) = \ln\left(\frac{4}{\pi}\right) - \frac{D_{eff}\pi^2}{4L^2} \quad (2)$$

$$\ln\left(1-\frac{A_t}{A_\infty}\right) = t \quad (3)$$

$$D_{eff} = \frac{m}{\pi^2 4L^2} \quad (4)$$

where A_t is the absorbance, A_∞ is the absorbance at equilibrium, and L is the thickness of the sample. A detailed description of the calculation and boundary conditions are given in Schampera and Dultz (2009).

The effective diffusion coefficient (D_{eff}) used here was defined by Shackelford and Daniel (1991) and includes the tortuosity factor. Diffusion measured in the in-diffusion experiment is controlled by boundary conditions such as tortuosity or the thickness of bound H_2O layers. Diffusion is also porosity and water-volume dependent for water-saturated and unsaturated samples, respectively. The apparent diffusion coefficient is also called the effective diffusion coefficient of a reactive solute (Gillham *et al.*, 1984). As non-reactive solutes were determined, the term 'effective diffusion coefficient' is used here.

Calculation of error of D_{eff}

Average values of D_{eff} from in-diffusion experiments were determined by 2−7 repetitions for each chosen experimental condition. The error in D_{eff} was calculated for the linear regression method by error propagation according to the Gauss equation 5

$$\frac{\Delta D_{eff}}{D_{eff}} = \sqrt{\left(\frac{E_a \cdot \Delta T}{R \cdot T^2}\right)^2 + \left(\frac{2 \cdot \Delta x}{x}\right)^2 + \left(\frac{2 \cdot \Delta b}{b}\right)^2} \quad (5)$$

where ΔD_{eff} is the error from an individual experiment of the D_{eff} value of the sample; E_a, the activation energy (7.8 kJ/mol according to Simonyan *et al.*, 2009, and Longsworth, 1960); T, the mean temperature (22.7ºC); ΔT, the deviation of the mean temperature; x, the height of the sample; Δx, the deviation of the mean height of the sample; b, the fitting parameter of the linear regression method; and Δb, the deviation of the mean fitting parameter. All other parameters, *e.g.* the point of measurement and the pressure, were kept constant during the experiment.

RESULTS AND DISCUSSION

Interlayer structure of organo-montmorillonites

While the d_{001} value of montmorillonite is 1.40 nm, the addition of organic cations in amounts corresponding to 40% of the CEC leads to basal spacings of 1.84, 1.52, and 1.42 nm for TPP-, BE-, and HDPy-montmorillonite, respectively (Figure 3). These basal spacings represent a monomolecular arrangement of the organic cations in the interlayer. Such small amounts of organic cations (*e.g.* 40% CEC) are almost completely exchanged, resulting in the same or similar uptake, whereas with greater amounts (*e.g.* 400% CEC) the uptake was much less (144, 191, and 222% CEC, respectively; Figure 3). The difference between applied and adsorbed amounts of organic cations can be deduced in more detail from the sorption isotherms (Figure 6).

For TPP-montmorillonites, the basal spacing, even with the largest amounts of TPP applied (400% CEC applied, 144% CEC uptake), is constant (1.80−1.84 nm). At loadings of TPP from 76% or more, the XRD maxima at 0.92 nm represent the second order (d_{002}) harmonic. Compared to the XRD pattern of the original montmorillonite, the structure factor for the adsorbed TPP is greater and impacts heavily on the peak intensity of d_{001}. The increase in the intensity of the d_{001} peak from TPP-40 to TPP-76, together with the formation of a second-order spacing indicates that the interlayer space is filled continuously up to loadings of 76% CEC. A continuous increase in the amount adsorbed in the interlayer space along with the amount applied can also be observed in the XRD patterns for the organo-clay combinations of BE and HDPy.

From the unit-cell dimensions of the BECl salt, which are 0.94 nm × 1.32 nm × 2.25 nm (Tanaka and Hirayana, 2008), d_{001} values of 1.6−1.7 nm were deduced for BE-montmorillonite with an organic monomolecular arrangement and 2.5−2.7 nm with a bimolecular arrangement in the interlayer space. In the XRD pattern of BE-montmorillonite with an uptake of 40−74% CEC, a continuous increase of the basal spacing from 1.52 to 2.01 nm was observed, indicating a poorly ordered arrangement in the interlayer space due to the complex structure of BE. For greater loadings (BE-102 to BE-191), diffraction maxima were observed at 2.60−2.68 nm. For BE-montmorillonite, a second-order XRD maximum occurs at 1.37 nm. Further discussion about the structure of BE in the interlayer space of montmorillonite would require speculation beyond data currently available in the literature.

With increasing amounts of HDPy, the basal spacing of MX-80 shifted to larger d values in three steps, also observed for other bentonites modified with long-chain organic cations (Zhu *et al.*, 2008): the basal spacing for

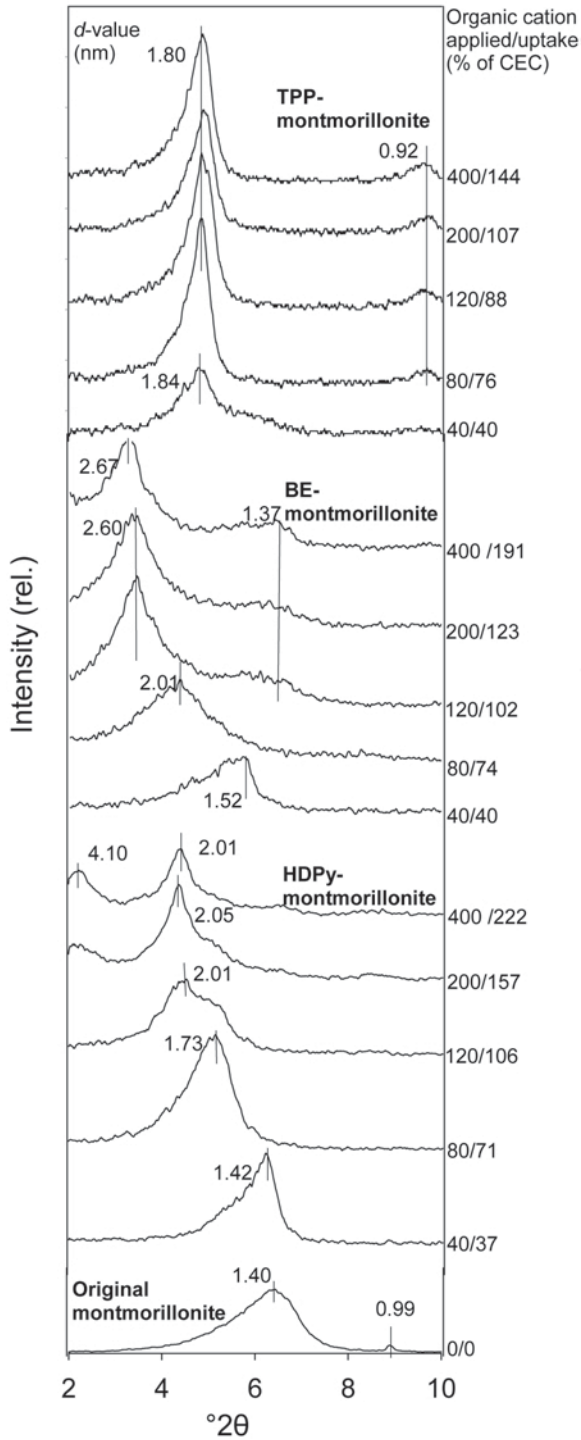

Figure 3. XRD patterns of HDPy-, BE-, and TPP-montmorillonite samples used in the diffusion experiments.

HDPy-montmorillonite at 1.42 nm represents a monomolecular arrangement; that at 1.7 nm, a bimolecular arrangement; and at 2.05 nm at high loadings, a pseudo-trimolecular arrangement (Meleshyn and Bunnenberg, 2006). Diffraction maxima at 4.1 nm may represent a superstructure, but also are interpreted as bilayer paraffin-like complexes (Koh *et al.*, 2005).

In the dry state with a d_{001} value of 0.98 nm, the solid density of montmorillonite is generally estimated to be 2.7 g/cm^3. As a consequence of the uptake of organic cations in the interlayer space, the solid density decreased to 2.27 g/cm^3 in the air-dry state (d_{001} of 1.42 nm). This greatly affects the final dry bulk density of the samples in the present diffusion experiments because a fixed amount of sample (7 mg) was used. The estimation of the solid density for HDPy-montmorillonites, where three different interlayer arrangements of the organic cation were observed, was based on structures determined by Monte Carlo simulations with differing contents of HDPy, Na, Cl, and H_2O in the interlayer space (Meleshyn and Bunnenberg, 2006). This calculation is based on the organic cation content per unit cell. In this model the interlayer cations are assumed to be distributed half on each of the two basal surfaces of the silicate layers bordering the interlayer space, but the organic cations on the external surface must also be considered. Calculations of the solid density for BE- and TPP-montmorillonites, where two (BE) and one (TPP) kind of organic-cation arrangement in the interlayer space is present, were, therefore, performed in the same way. The calculated results must be considered as estimates only, however, because no supporting molecular data are available for these organo-clay combinations.

HDPy-120, with a basal spacing of 2.05 nm, has a solid density of 1.73 g/cm^3. The smallest solid density calculated with 1.31 g/cm^3 for BE-154 shows a basal spacing of 2.68 nm. For TPP-montmorillonites, with basal spacing of 1.80 nm, the range of solid density is small from 1.62 g/cm^3 for TPP-40 to 1.82 g/cm^3 for TPP-84 to TPP-144 with increasing uptake of the organic cation.

The uptake of organic cations in the interlayer space of montmorillonite results in a marked increase in the basal spacings, which greatly affects the solid density of the clay platelets. In addition, the shape of the particles is changed by an increased thickness of the platelets, which may change the pore morphology of the compacted clays. Furthermore, the compressibility of bentonite is affected by the uptake of organic cations in the interlayer space by up to one order of magnitude of the compression index (Soule and Burns, 2001).

Surface charge

The negative charge of the external surfaces of the original bentonite, quantified by polyelectrolyte titration, was 99.5 mmol$_c$/kg (Figure 4), which is ~14% of the CEC (0.86 mol$_c$ kg^{-1}). Through the addition of organic cations in incremental amounts of 2% of the CEC, a strong increase in SC was observed, indicating that organic cations are preferentially adsorbed on the external surfaces. For all three organo-clay combina-

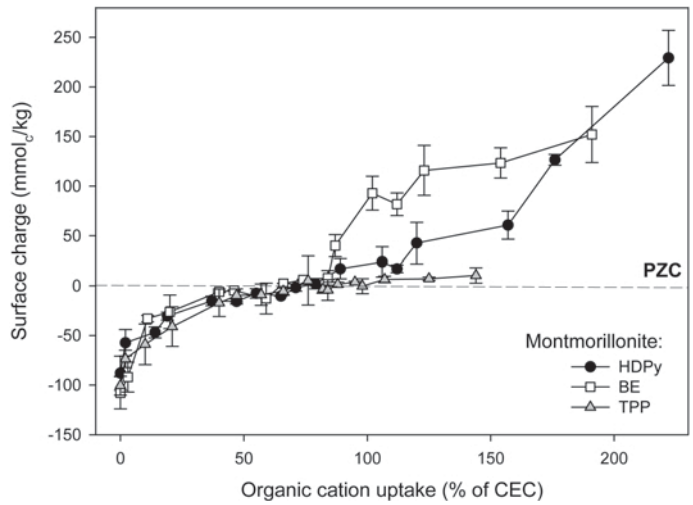

Figure 4. Surface charge of HDPy-, BE-, and TPP-montmorillonite depending on the uptake of organic cations.

tions, the increasing trend in SC was similar until the PZC was reached, indicating that negative SC is neutralized by all three organic cations in the same way.

The PZC was reached when the uptake of organic cations was at 74% CEC for TPP, 82% CEC for BE, and 79% CEC for HDPy, respectively. At the PZC, >90% of the applied organic cations were adsorbed. Above the PZC, at greater loadings of organic cations, the three organo-clays showed marked differences in SC. For TPP-montmorillonite, even at the highest loadings (144% CEC uptake of TPP), the SC was only slightly reversed from negative to positive (10.4 mmol$_c$/kg), while BE- and HDPy-montmorillonites showed a much larger uptake of organic cations (191% and 222% CEC uptake for BE and HDPy, respectively) with a corresponding increase in net positive SC (152.1 and 230.5 mmol$_c$/kg, respectively). With increasing uptake of organic cations, the SC became more positive because the number of binding sites in the interlayer space was limited and greater amounts of organic cations were adsorbed on the external surfaces, exceeding the CEC. This phenomenon evidently depends on the structure of the organic cation. Above the PZC, at the same levels of organic cation uptake, the SC of BE-montmorillonite increased more than did that of HDPy-montmorillonite. Such behavior is attributed to the fact that HDPy first forms incomplete monolayers on the external surfaces of montmorillonite (Meleshyn, 2009), where the positively charged pyridinium rings are adsorbed on the clay surface and the uncharged alkyl chains are oriented perpendicular to the basal plane. When the monolayer is completed, HDPy cations form a second layer where the positively charged pyridinium rings are exposed to the aqueous phase inducing an increase in SC at greater loadings. The initial increase in SC above the PZC of BE-montmorillonite is due to the fact that the complex structure of the BE cation hinders the formation of an ordered organic layer on the external surfaces, inducing the exposure of positive charge to the solution.

The structure of the organic cations plays an important role in the range of positive SC where bilayer formation occurs for HDPy and BE cations, while TPP cations build a monolayer with just some TPP cations in a second incomplete layer on the external surfaces (Jeschke and Meleshyn, 2010). The largest positive SC was observed in HDPy-montmorillonite, with 230.5 mmol$_c$/kg, whereas it was smallest for TPP-montmorillonites, with a maximum value of 10.4 mmol$_c$/kg. The observed variability in the SC measurements, which for the original bentonite is −85 to −108 mmol$_c$/kg, is due to the completeness of clay dispersion and to the titration method used to measure it. Measurement of surface-charge values just below the PZC using the polyelectrolyte method sometimes overestimates the SC.

Wettability

For HDPy- and BE-montmorillonite a marked increase in Θ by the uptake of organic cations was obtained (Figure 5). A maximum Θ for all these organo-clays was observed when the organic-cation uptake was ~40% CEC. For HDPy-9 to HDPy-55, Θ >90º was determined, indicating hydrophobic surface properties. Remarkably, the largest Θ values were obtained for samples having a slightly negative SC (−46.9 to −7.6 mmol$_c$/kg). HDPy-71, which is at the PZC, had Θ = 74º. With increasing positive SC, a further decrease of the contact angle was observed. Almost the same wettability as the original sample (Θ 53º) was obtained for HDPy-157 with Θ = 48º. At greater loadings with HDPy (sample HDPy-110 to -222), Θ was similar (~40º).

Despite the increase in Θ (>65º) for BE-montmorillonite at low loadings, all samples exhibited

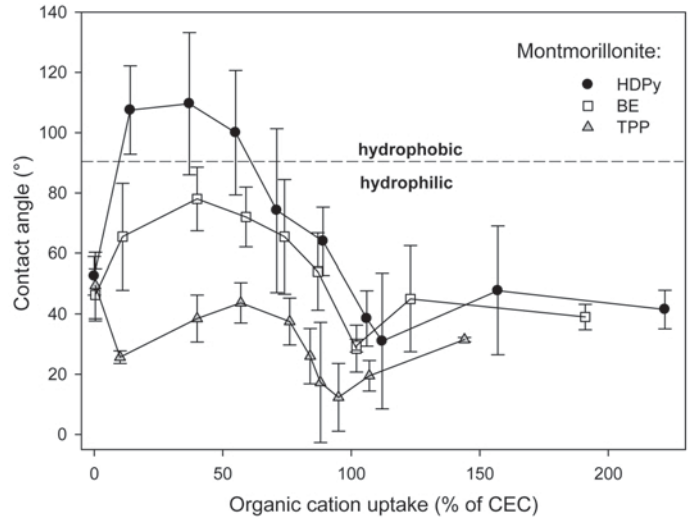

Figure 5. Contact angle of HDPy-, BE-, and TPP-montmorillonite depending on the uptake of organic cations.

hydrophilic surface properties. The Θ value of BE-montmorillonite varied between 29º and 78º. Similar to the HDPy-montmorillonite, the largest Θ value coincided with slightly negative SC values and the trend of Θ at higher loadings was comparable. The smallest values for Θ, varying from 12º to 44º, were obtained for TPP-montmorillonite (Figure 5), indicating strongly hydrophilic properties.

Organic cation distribution between external surfaces and the interlayer space

Comparing the amount of organic cation applied with the amount adsorbed (Figure 6) reveals that the organic cations were almost totally adsorbed for HDPy up to 120% CEC applied, while for BE and TPP the corresponding values were 100% and 80% CEC, respectively. As organic-cation sorption increased, the properties of the organo-clays changed, depending on the cation. For example, the cations behave differently with respect to their distribution between the interlayer and external surfaces and in their degree of organization at the basal surfaces. In order to compare the effects of the organic cations' organo-clay properties, and to provide additional background information for the diffusion experiments, a scheme illustrating changes in organo-clay properties was added to the sorption isotherms (Figure 6) to show simultaneous changes in SC, hydrophobicity *vs*. hydrophilicity (Θ), and cation orientation and configuration at the silicate surface.

The SC and the wettability of the organo-clay samples were affected by the arrangement of organic and inorganic cations adsorbed on clay particle surfaces. Marked changes in SC and Θ of the organo-clays at 2−10% organic cations of CEC applied indicated that considerable amounts were adsorbed on the external surfaces. According to SC measurements on the original bentonite, as many as 14% of the cation exchange sites are located on the external surfaces, indicating that organic cations in amounts up to 14% CEC could be adsorbed on external surfaces.

At low applied amounts, the typical arrangement of HDPy on the surface of montmorillonite is as a monolayer (Meleshyn, 2009). Spectroscopic results show that micelle-like surfactant aggregate clusters form on the surface (Kung and Hayes, 1993). As the positively charged pyridinium ring adsorbed onto the clay mineral surface, the negative charge of the silicate layer was effectively neutralized and the hydrophobic alkyl chains project into the interlayer, perpendicular to the basal plane. The formation of such monolayers can explain the observed hydrophobic properties of HDPy-montmorillonite.

The highest Θ values were found in samples with a slightly negative SC and not at the PZC, probably due to the initial stages of the formation of a second layer of HDPy cations where the cation was rotated by 180º so the alkyl chain points toward the surface of montmorillonite and the alkyl chains in the first layer, whereas the positively charged pyridinium ring is exposed to the aqueous phase. As a consequence of this bilayer formation, the surface became more hydrophilic. The PZC was defined as the point where the sum of positive and negative charge is zero. Therefore, strong positive SC and hydrophilic surface properties at greater loadings with HDPy indicate the formation of bilayer structures.

The increase in Θ at low loadings of BE is due to uncharged alkyl chains and aromatic rings which are oriented away from the surface of montmorillonite, while the positively charged nitrogen ion is adsorbed. The strong increase in SC with greater BE loading indicates the formation of a more or less ordered bilayer

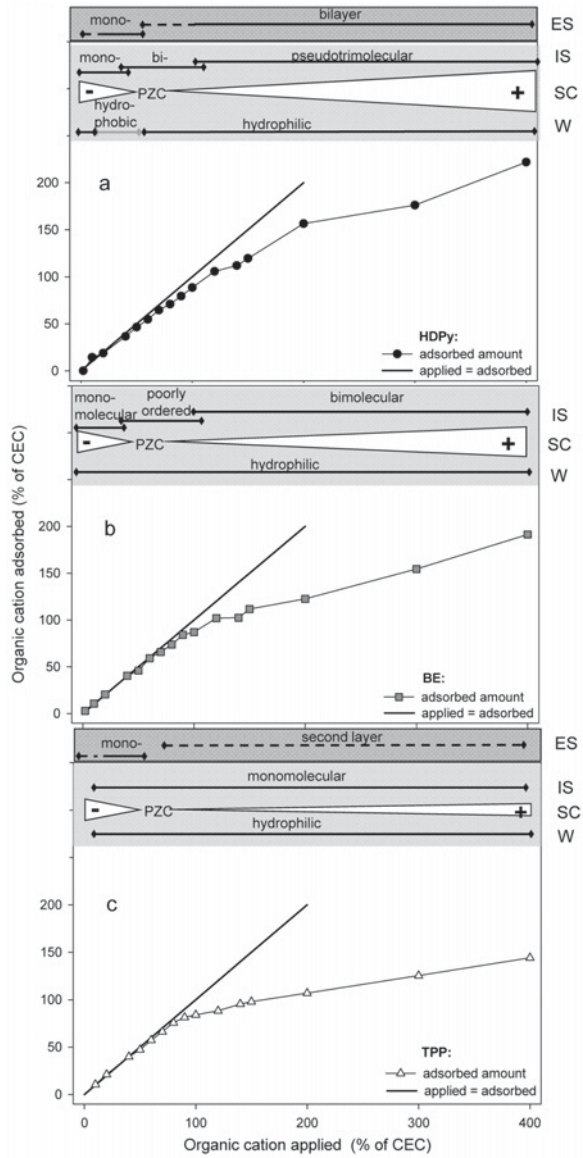

Figure 6. Comparison of the applied and adsorbed amount of organic cations for the organo-clay combinations with (a) HDPy, (b) BE, and (c) TPP. To understand the material properties in the diffusion experiments better a scheme for cross interpretation between organic cation uptake and material properties, variability in the structure on the external surfaces (ES) and in the interlayer space (IS), the surface charge (SC), and the wettability (W) were added.

structure. Some hindering of ideal layered arrangement of BE cations in the interlayer space, which builds up continuously rather than stepwise, is also evident from XRD analysis (Figure 3).

For TPP-montmorillonite, the basal spacing is constant at 1.8 nm for all amounts of TPP applied, limiting further uptake of organic cations in the interlayer space. Thus, a continuous increase in the amount of TPP on the external surfaces can be assumed. The fact that the SC is slightly positive and near the PZC even at greater loadings indicates that the positive charge of TPP is effectively compensated by counter anions (presence of ion pairs). From the aggregation behavior of TPP-montmorillonite, Patel *et al.* (2007) concluded that TPP with its cyclic phenyl groups covers the surface of a platelet to a smaller degree compared with longer-chained organic cations. Hence, TPP can easily be adsorbed on the surface of montmorillonite forming 1−2 loose layers. The small contact angle for TPP-montmorillonites indicates the presence of charged sites and/or H_2O in the TPP-layer on the external surfaces.

The formation of bound H_2O layers, which influence the wettability, depends on the amount and steric arrangement of organic cations, inorganic cations, and ion pairs on the external surface. The observed hydrophobic properties of HDPy-montmorillonite with Θ >90º are due to monolayers with hydrophobic alkyl chains oriented perpendicular to the basal plane of montmorillonite, thus preventing the formation of bound H_2O layers. The other organo-clays used here with Θ between 15 and 78º also have water-repellent properties but are not as hydrophobic as the HDPy-montmorillonite. Their distinct hydrophilic properties allow the formation of bound H_2O layers which increase the apparent volume of the clay particles and hinder the diffusion process.

Calculation of the diffusion coefficient

The exchange of D_2O by H_2O during the diffusion experiment in the D_2O-saturated samples was clearly traceable in the IR spectra by the increased absorbance of the O−H stretching vibration at 3380 cm^{-1} and the simultaneous decrease in the O−D stretching vibration at 2480 cm^{-1} (Figure 7), measured at the contact interface of the sample with the diamond window of the ATR unit.

The increased absorbance of the asymmetric CH_2 stretching vibration at 2965 cm^{-1} from the organic cation indicates that the amount of sample detectable by the IR beam increased during the experiment, probably due to some compression settling and/or to some variation in the baseline intensity.

The decreased absorbance of the CO_2 stretching vibration (asymmetric) at 2350 cm^{-1} indicated that during this experiment the CO_2 content in the laboratory atmosphere was changing (over the 20 h period of the experiment).

A short overview of the plots used for the determination of D_{eff} of three samples with strong differences in the time-dependent increase in absorbance (HDPy-37, BE-40, and TPP-40) (more details can be found in Schampera and Dultz, 2009) revealed that the largest value for D_{eff} was obtained from sample HDPy-37, the sample with the strongest hydrophobic surface properties. The values for D_{eff} calculated from the increased absorbance of the O−H stretching vibration for samples with the same amount of applied organic cation varied

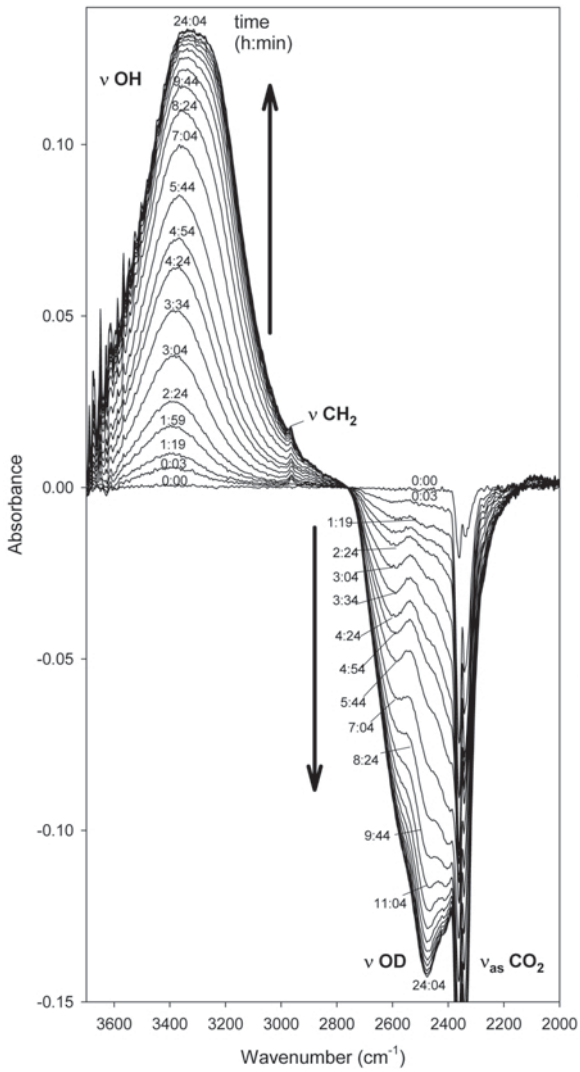

Figure 7. Change of the absorbance of the O–H and O–D stretching vibrations during a $H_2O \rightarrow D_2O$ exchange experiment with D_2O-saturated BE-montmorillonite (BE uptake: 123% CEC). The dry bulk density of the sample was 1.21 g/cm^3.

between 6.4×10^{-11} m^2/s (HDPy-37), 2.1×10^{-11} m^2/s (BE-40); and 9.2×10^{-12} m^2/s (TPP-40, Figure 8). The best-fit linear regression lines (Figure 8, equations 2 and 3) consistently gave $r^2 = 0.99$.

In general, the standard error did not exceed 7%. In a very limited number of diffusion experiments the increase in absorbance occurred stepwise, probably due to some heterogeneity in the organization of particles in the clay platelets, resulting in a greater standard error of up to 25%.

Systematic effect of density and degree of saturation on D_{eff}

For the original bentonite in the saturated state, D_{eff} in the high dry bulk density range was considerably smaller ($2.4 \times 10^{-11} \pm 5.6 \times 10^{-12}$ m^2/s) than in the low dry bulk density range ($6.7 \times 10^{-11} \pm 4.5 \times 10^{-12}$ m^2/s) (Figure 8). The smaller D_{eff} was due to the decrease in pore volume and shift to smaller pore sizes at greater dry bulk density (Hicher *et al.*, 2000; Jougnot and Revil, 2007). Here, also, a compression of the clay platelets combined with a release of water must be considered. At a dry bulk density of 1.3 g/cm^3, three water layers are present in the interlayer space of bentonite whereas only one water layer is present at a dry bulk density of 1.8 g/cm^3 (Van Loon *et al.*, 2007).

The effect of the experimental conditions on D_{eff} for BE-montmorillonites (Figure 9) revealed results that were typical for all hydrophilic organo-clay samples under investigation. Like BE-montmorillonites, all TPP- and HDPy-montmorillonites, with the exception of the hydrophobic sample HDPy-37, behaved in the same way. For hydrophilic samples, the D_{eff} was retarded by an increase in dry bulk density (Figure 11) and a decrease in the degree of water saturation (Figure 13).

As already mentioned, organic cations adsorbed on the external surfaces, together with bound H_2O layers, decreased diffusive transport by increasing the apparent volume of the clay platelets and narrowing the diffusion pathways. With increasing amounts of BE applied, the value of D_{eff} is always smaller under the experimental conditions than that of the original bentonite. Despite some increase in Θ at low loadings, the presence of organic cations together with bound H_2O on the external surfaces affected the observed decrease in D_{eff}. Some increase in D_{eff} was observed for BE-191, the sample with the greatest loading under all three experimental conditions. For this sample, large positive SC values indicated considerable amounts of organic cations on the external surfaces, which might hinder the formation of dense packing of clay platelets.

For BE-102, a minimum in D_{eff} was observed under all three experimental conditions. The low solid density of BE-102 (1.33 g/cm^3) may lead to a greater dry bulk density when the interlayers are compressed by the applied pressure. Bimolecular arrangements in the interlayer space are more sensitive to mechanical load than monomolecular arrangements (Mazo *et al.*, 2008). As BE-102 had the smallest C content compared to other BE-montmorillonites, having a bimolecular arrangements in the interlayer space, a high sensitivity to mechanical stress resulting in a greater compressibility was probable and may explain the typical minimum for D_{eff}.

Effect of bound H_2O layers on D_{eff}

The value for D_{eff} was similar for all three organo-clay combinations if in the low-density range under water-saturated conditions (Figure 10a). The adsorption of organic cations decreased the D_{eff} by ~0.5 orders of magnitude compared to the original montmorillonite (Figure 10a), due to the fact that organic-cation

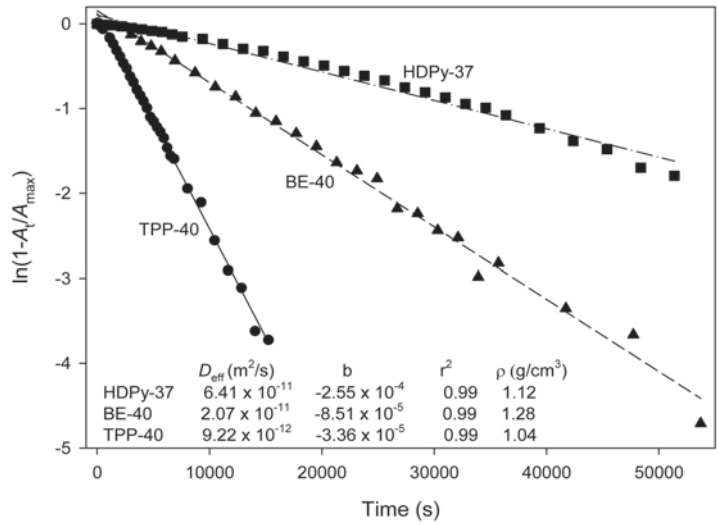

Figure 8. Illustration of the calculation of D_{eff} by the linear regression method for samples HDPy-37, BE-40, and TPP-40 with marked differences in the increase of the absorbance of the O−H stretching vibration with time. Experiments at water-saturated conditions and bulk densities from 1.04 to 1.28 g/cm^3. The symbols represent D_{eff} calculated by equations 2 and 3 and then plotted *vs.* time and are shown together with the linear regression and gradient b.

adsorption on the external surfaces increased the apparent volume of the platelets. The effects of the hydrophobic surface properties of sample HDPy-37 were not detected.

At partial water saturation (Figure 10b), relatively small values for D_{eff} were obtained and no systematic differences were observed among the three organo-clay combinations. The small water volume affects the diffusive transport significantly, and the observed differences in D_{eff} were not related to surface properties such as SC and Θ.

Only in the high dry bulk density range and under water-saturated conditions (Figure 10c) did the hydrophobic surface properties of sample HDPy-37 result in a notably larger value for D_{eff} (2.7×10^{-10} m^2/s) compared to 2.4×10^{-11} m^2/s for the original montmorillonite. The smallest values for D_{eff} (5.9×10^{-12} m^2/s) were found in the hydrophilic sample TPP-76. Compared to HDPy-37, the difference in the D_{eff} was >1 order of magnitude. For TPP-40 a relatively small value (9.1×10^{-12} m^2/s) was obtained. For BE-40, D_{eff} was 1.7×10^{-11} m^2/s, a value intermediate between HDPy- and TPP-montmorillonite. At an organic-cation uptake >102% CEC all three organo-clay combinations had comparable D_{eff} values.

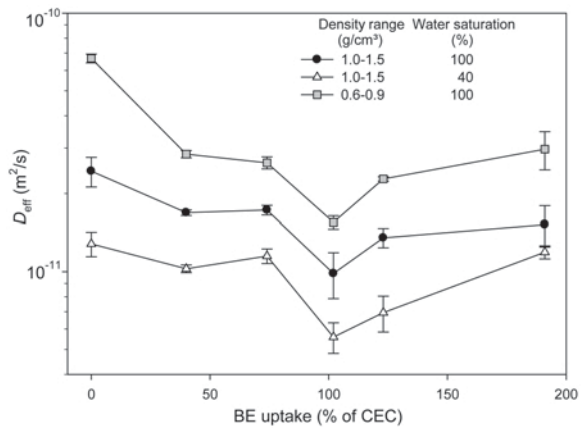

Figure 9. Effect of water saturation (40 and 100%) and dry bulk density on D_{eff} of BE-montmorillonite with a BE uptake of 0−144% CEC.

Surface properties influenced D_{eff} at large bulk density values with small pore sizes. Under these conditions, bound H_2O layers were effective as obstacles to diffusion by narrowing the diffusion pathways of free water. Notable differences between the three organo-clay combinations were observed if the amount of organic cations applied was $\leqslant$80% CEC. At applied amounts >80% CEC, the different organo-clay combinations had almost the same effect on D_{eff}.

In the high dry bulk density range (Figure 10c), the observed variability of D_{eff} at low loadings with organic cations can be related to the contact angle of the samples (Figure 5). The hydrophobic sample HDPy-37 had the largest D_{eff} value whereas the hydrophilic sample TPP-40 had the smallest. Sample BE-40 was intermediate. The absence of bound H_2O in the pores seemed to accelerate the diffusive transport. The small Θ value for TPP-40 indicated hydrophilic surface properties; consequently, strongly bound H_2O layers explain the observed small D_{eff} value. The hydrophilic surface immobilized water at the sample surface and thus reduced the effective pore diameter for diffusive transport.

At higher loadings of organic cations ($\geqslant$100% CEC) all samples had small Θ values, indicating hydrophilic

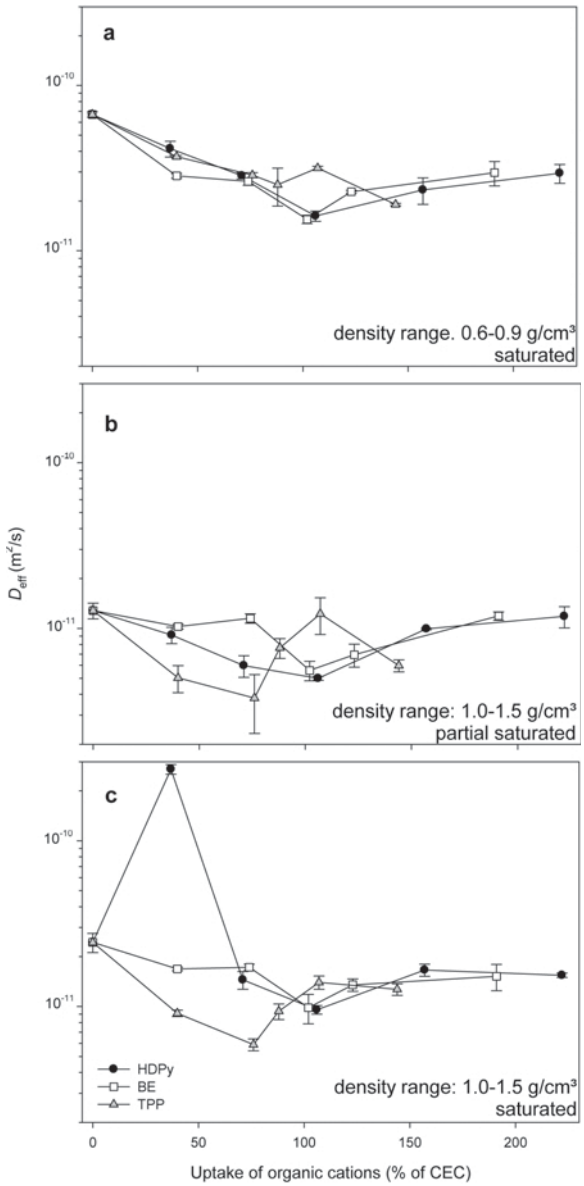

Figure 10. Change of D_{eff} of HDPy-, BE-, and TPP-montmorillonite with increasing amounts of organic cation applied. Samples were water-saturated in the low dry bulk density range of 0.6−0.9 g/cm^3 (a), partially water saturated (~40%) in the high dry bulk density range of 1.0-1.5 g/cm^3 (b), and water-saturated in the high dry bulk density range of 1.0−1.5 g/cm^3 (c).

surface properties. In addition to bound H_2O layers, layers of organic cations on the external surfaces narrowed the diffusion pathways and, therefore, D_{eff} for these samples is somewhat less than for the original bentonite.

Another effect at high loadings with organic cations is the change in the clay particle thickness by the uptake of organic cations in the interlayer, which resulted in a considerable expansion of d_{001} values to 1.8−2.67 nm (Figure 3), which affected the pore geometry and, therefore, the tortuosity. A compression of the interlayer, combined with a loss of interlayer water due to the applied pressure, is known for bentonite (Van Loon *et al.*, 2007) and organo-clays (Mazo *et al.*, 2008). As a consequence of compression and also the orientation of clay platelets at high applied pressure (Schampera and Dultz, 2009), the accessible pore volume can decrease, the tortuosity increase, and the diffusive transport be retarded. As already described, besides a decrease in pore volume at high pressures, a shift to smaller pore sizes occurs, increasing the effect of bound H_2O layers on diffusive transport (Delage *et al.*, 2006).

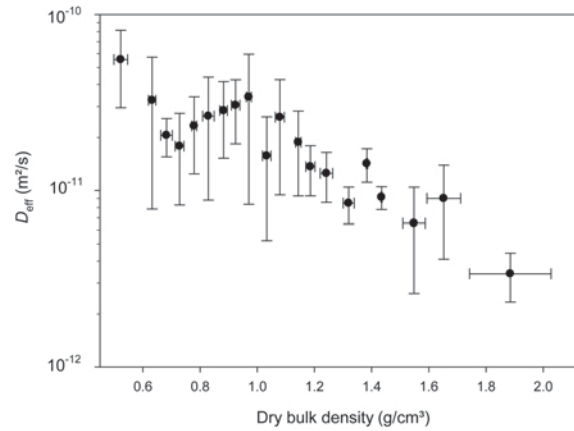

Figure 11. Effect of dry bulk density on D_{eff} of all 109 hydrophilic samples measured at water-saturation.

The relation between dry bulk density and D_{eff} under water-saturated conditions was plotted for all 109 hydrophilic samples (Figure 11). The results define a smooth curve but can also be interpreted by a linear trend. In the dry bulk density range from 0.5 to 1.2 g/cm^3, only a small decrease in D_{eff} was observed from 5.6×10^{-11} to 1.9×10^{-11} m^2/s. For the decrease in dry bulk density from 1.2 to 1.9 g/cm^3, the difference was an order of magnitude, from 1.4×10^{-11} to 3.4×10^{-12} m^2/s.

To remove the effect of solid density on the platelet volume of the organo-clay combinations, the pore volume calculated from either the bulk density or the solid density was plotted *vs.* D_{eff} (Figure 12). The differences between the plots can be attributed to the effects of surface properties. For all organo-clay combinations in the water-saturated or partially water-saturated state, an increase in D_{eff} was observed with pore volume. The hydrophobic sample HDPy-37, already visible in Figure 10c, had a markedly larger D_{eff} value. The BE-montmorillonite sample BE-191 yielded a slightly larger D_{eff} value, which cannot be explained by the wettability of the sample and may be related to the microstructure.

To show the effect of interconnections within the water network on D_{eff}, the water volume of the samples was calculated from porosity and degree of water

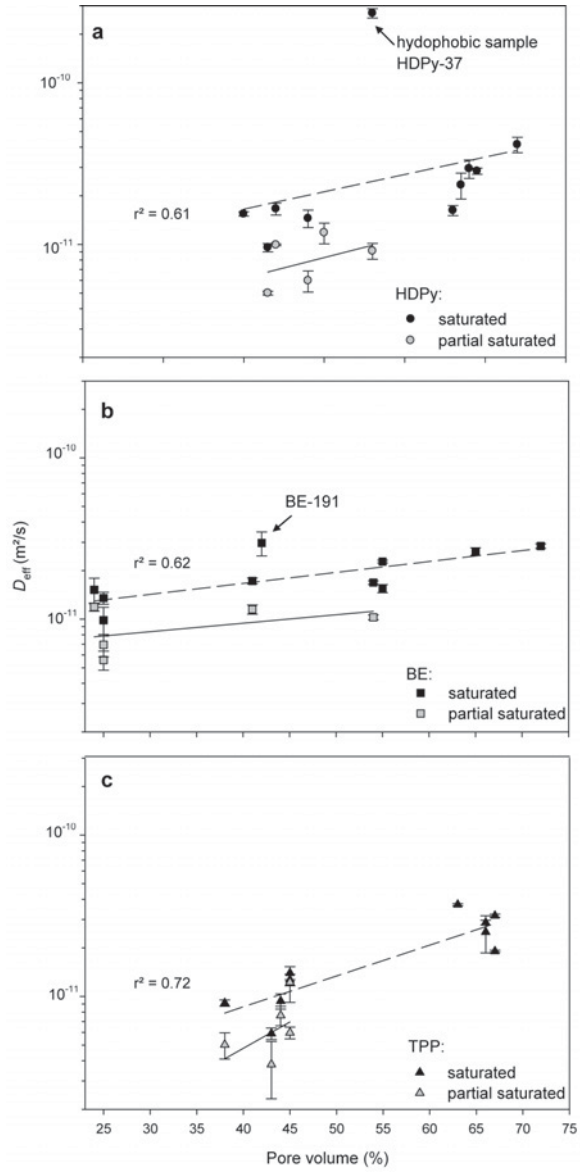

Figure 12. Effect of pore volume on D_{eff} for (a) HDPy-, (b) BE-, and (c) TPP-montmorillonite fully and partially water-saturated. Coefficients of determination (r^2) are shown for data measured at water-saturation only. Note that D_{eff} of the hydrophobic sample HDPy-37 and sample BE-191 determined under water-saturated conditions are not included in the calculation of the linear regression line.

saturation of the samples. From the plot of D_{eff} for all partially and fully water-saturated samples shown in Figure 12a–c *vs.* the water volume, a single, linear relationship was obtained for all hydrophilic samples (Figure 13). D_{eff} increased with the water volume. This argues in favor of the existence of good interconnections within unsaturated (partially saturated) samples. An exception is again the hydrophobic sample HDPy-37 where diffusive transport at a comparable water volume is much faster.

Verification of the quantitative aspect of the method

The analyzed D_{eff} values agree with those obtained in classical diffusion studies. Similar to the present results, Bourg *et al.* (2006) reported, based on the evaluation of ten studies on diffusion transport in compacted Na-bentonites, a decreasing value for D_{eff} of water molecules with increasing dry bulk density, from ~1×10^{-9} m^2/s at a density of 0.2 g/cm^3 to ~1×10^{-11} m^2/s at a density of 2.0 g/cm^3. At a density of 1 g/cm^3, for example, D_{eff} varied between 1×10^{-10} and 5×10^{-10} m^2/s, while at a density of 1.5 g/cm, D_{eff} varied between 2×10^{-10} and 2×10^{-11} m^2/s. The variation at lower density was one order of magnitude greater than at higher density. For very low density (<0.2 g/cm^3), the D_{eff} value almost reached that of free water, which was 2.3×10^{-9} m^2/s (Mills, 1973). These results and observations showed that D_{eff} was controlled by the pore network geometry.

With the same method, slightly smaller values for D_{eff} of between 6.5×10^{-11} and 7.2×10^{-11} m^2/s were found on powder/pellet-bentonites with bulk densities of 1.25–1.39 g/cm^3 (Garcia-Gutierrez *et al.*, 2004). This could explain the variation of the error in D_{eff} under comparable conditions. The relation between D_{eff} and the moisture content is well known (Hunt and Ewing, 2003).

The fracture planes of pellets used for diffusion experiments in the high dry bulk density range revealed a high degree of orientation perpendicular to the applied pressure, whereas in the low dry bulk density range, no preferred orientation was visible (Schampera and Dultz, 2009). Due to the preferred orientation of clay platelets in the high dry bulk density range, together with a decrease in pore volume and shift in pore-size distribution, D_{eff} decreased. In diffusion experiments the importance of the orientation of particles was shown, as D_{eff} was larger if the platelets were oriented parallel than if they were perpendicular to one another (Yllera *et al.*, 2004). Besides particle orientation, pore volume and pore-size distribution also have a decisive role in determining diffusive transport (Delage *et al.*, 2006).

If the organo-clay has a low dry bulk density, pore geometry has the main influence on D_{eff}, whereas at high bulk density, bound H_2O layers are the main influence. If the density is intermediate, both may assert their influence. Different gradients for the decrease in D_{eff} in the dry bulk density range from 0.5 to 1.2 g/cm^3 and 1.2 to 1.9 g/cm^3 may also be related to the shift in pore size from more pores between aggregates to more between the clay platelets, as with smaller pore size the influence of bound H_2O increases.

CONCLUSIONS

Determination of diffusive transport by ATR-FTIR is a fast and precise method for analyzing clays for their

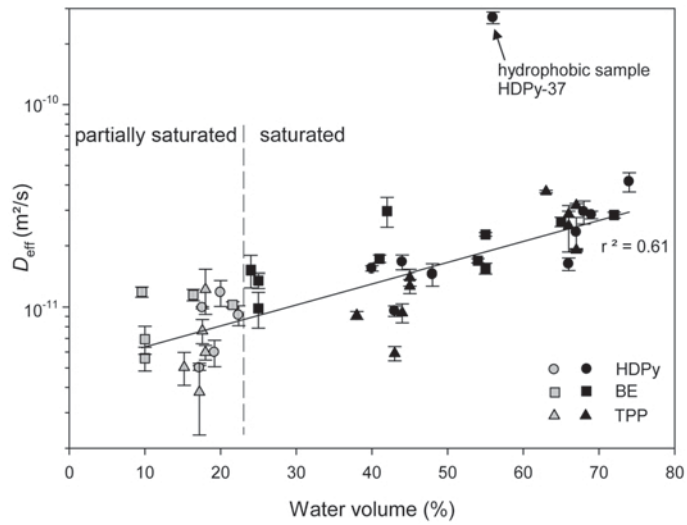

Figure 13. Effect of water volume on D_{eff} for partially and fully water-saturated HDPy-, BE-, and TPP-montmorillonite. Note that D_{eff} of the hydrophobic sample HDPy-37 determined under water-saturated conditions are not included in the calculation of the linear regression line.

applicability in engineered barriers. Larger diffusion cells which allow a more accurate determination of the compaction rate can be built if a multiple-reflection ATR accessory is used. In this case, the absorbance of the O−H stretching vibration is multiplied, which allows better quantification of diffusive transport. Values for D_{eff} derived by this method were comparable to those obtained by more common laboratory-scale methods. The results show that the configuration of this in-diffusion experiment allows the determination of the pore volume for water-saturated samples and the water volume for both the partially and fully water-saturated samples.

Variations of dry bulk densities and porosities due to different solid densities of the organo-clay samples can be avoided if the solid densities are known accurately and considered during preparation of the clay pellet. This is imperative if more reliable comparisons between the different diffusion experiments are to be obtained.

Organic cations adsorbed on the external surfaces of bentonite narrow the diffusion pathways and decrease the diffusive transport. For hydrophilic organo-clays, D_{eff} is always less than that of the original bentonite. Hydrophobic surface properties, which could severely increase D_{eff}, were observed only for HDPy-montmorillonite as a result of monolayer arrangements of the organic cations on the external surfaces. From the viewpoint of diffusive transport, the use of hydrophilic organo-clays in barrier systems is expected, therefore, to increase the sorption capability for neutral and anionic compounds. This is substantiated by the fact that the organic cations have a high selectivity for the exchange sites of the clay minerals compared to the major cations in groundwater.

The structure of the organic cation is important in preparing the organo-clay for the desired anion adsorption capability and other surface properties which affect diffusive transport. Because hydrophobic surfaces, for example, increase the diffusive transport under certain conditions, special attention must be given to the structure of the organic cations used for the preparation of organo-clays. The use of modeling for the identification of suitable structures of organic cations also has to be considered.

ACKNOWLEDGMENTS

The authors thank J. Janowitz and M. Below for their skilful assistance in the laboratory. They are also grateful to A. Meleshyn (Institute for Radioecology and Radiation Protection, Leibniz University Hannover) for help with programming, and to H. Behrens (Institute of Mineralogy, Leibniz University Hannover) and J.B. Percival (Geological Survey of Canada) for valuable discussions. This study was supported by the Bundesministerium für Wirtschaft und Technologie (BMWi) under contract number 02E 10025.

REFERENCES

An, J.-H. and Dultz, S. (2007) Adsorption of tannic acid on chitosan-montmorillonite as a function of pH and surface charge properties. *Applied Clay Science*, **36**, 256−264.

Bachmann, J., Woche, S.K., Goebel, M.-O., Kirkham, M.B., and Horton, R. (2003) Extended methodology for determining wetting properties of porous media. *Water Resources Research*, **39**, article no. 1353.

Böckenhoff, K. and Fischer, W.R. (2001) Determination of electrokinetic charge with a particle-charge detector and its relationship to the total charge. *Fresenius Journal of Analytical Chemistry*, **371**, 670−674.

Bors, J., Gorny, A., and Dultz, St. (1997) Iodide, caesium and strontium adsorption by organophilic vermiculite. *Clay Minerals*, **32**, 21−28.

Bors, J., Dultz, S., and Riebe, B. (2000) Organophilic bentonites as adsorbents for radionuclides I. Adsorption of ionic fission products. *Applied Clay Science*, **16**, 1−13.

Bourg, I.C., Sposito, G., and Bourg, A.C.M. (2006) Tracer diffusion in compacted, water-saturated bentonite. *Clays and Clay Minerals*, **54**, 363–374.

Boving, T.B. and Grathwohl, P. (2001) Tracer diffusion coefficient in sedimentary rocks: correlation to porosity and hydraulic conductivity. *Journal of Contaminant Hydrology*, **53**, 85–100.

Chatterjee, A., Iwasaki, T., Ebina, T., and Hayashi, H. (1997) Quantum chemical calculation on clay-water interface. *Applied Surface Science*, **121/122**, 167–170.

Delage, P., Marcial, D., Cui, Y.J., and Ruiz, X. (2006) Ageing effects in compacted bentonite: a microstructure approach. *Géotechnique*, **56**, 291–304.

Duval, F.P., Porion, P., Faugère, A.-M., and Van Damme, H. (2001) An NMR investigation of water self-diffusion and relaxation rates in controlled ionic strength laponite sols and gels. *Journal of Colloid and Interface Science*, **242**, 319–326.

Fielderson, G.T. and Barbari, T.A. (1993) The use of FTi.r.-a.t.r spectroscopy to characterize penetrant diffusion in polymers. *Polymer*, **34**, 1146–1153.

Garcia-Gutierrez, M., Mingarro, M., Missana, T., Martin, P.L., Sedano, L.A., and Cormenzana, J.L. (2004) Diffusion experiments with compacted powder/pellets clay mixtures. *Applied Clay Science*, **26**, 57–64.

Gillham, R.W., Robin, M.J.L., Dytynyshyn, D.J., and Johnston, H.M. (1984) Diffusion of nonreactive and reactive solutes through fine-grained barrier material. *Canadian Geotechnical Journal*, **23**, 541–550.

Guegan, R., Gautier, M., Beny, J.-M., and Mueller, F. (2009) Adsorption of a $C_{10}E_3$ non-ionic surfactant on a Ca-smectite. *Clays and Clay Minerals*, **57**, 502–509.

Hicher, P.Y., Wahyudi, H., and Tessier, D. (2000) Microstructural analysis of inherent and induced anisotropy in clay. *Mechanics of Cohesive-Frictional Materials*, **5**, 341–371.

Hunt, A.G. and Ewing, R.P. (2003) On the vanishing of solute diffusion in porous media at a threshold moisture content. *Soil Science Society of America Journal*, **67**, 1701–1702.

Hunter, R. (1993) *Introduction to Modern Colloid Science*. Oxford University Press, Oxford, UK, 338 pp.

Ichikawa, Y., Kawamura, K., Nakano, M., Kitayama, K., and Kawamura, H. (1999) Unified molecular and homogenization analysis for bentonite behaviour: current results and future possibilities. *Engineering Geology*, **54**, 21–32.

Ichikawa, Y., Kawamura, K., Nakano, M., Kitayama, K., Seiki, T., and Theramast, N. (2001) Seepage and consolidation of bentonite saturated with pure- or salt water by method of unified molecular dynamics and homogenization analysis. *Engineering Geology*, **60**, 127–138.

Imai, Y., Nishimura, S., Inukai, Y., and Tateyama, H. (2003) Differences in quasicrystals of smectite-cationic surfactant complexes due to head group structures. *Clays and Clay Minerals*, **51**, 162–167.

Jeschke, F. and Meleshyn, A. (2010) A Monte Carlo study of interlayer and surface structures of tetraphenyl-phosphonium-modified Na-montmorillonite. *Geoderma* (in press).

Johnston, C.T. and Tombacz, E. (2002) Surface chemistry of minerals. Pp. 37–67 in: *Soil Mineralogy with Environmental Applications* (J.B. Dixon and D.G. Schulze, editors). SSSA Book Series, no. **7**, Soil Science Society of America, Madison, Wisconsin, USA.

Jougnot, D. and Revil, A. (2007) Diffusion of ions in unsaturated clay-rocks: theory and application to the Callovo-Oxfordian argillite. International Meeting on Clay in Natural and Engineered Barriers for Radioactive Waste Confinement, Lille, France, pp. 247–248.

Koh, S.M., Song, M.S., and Takagi, T. (2005) Mineralogy, chemical characteristics and stabilities of Cetylpyridinium-exchange smectite. *Clay Minerals*, **40**, 213–222.

Kozaki, T., Inada, K., Sato, S., and Ohashi, H. (2001) Diffusion mechanism of chloride ions in sodium montmorillonite. *Journal of Contaminant Hydrology*, **47**, 159–170.

Kung, K.-H.S. and Hayes, K.F. (1993) Fourier transform infrared spectroscopic study of adsorption of cetyltrimethylammonium bromide and cetylpyridinium chloride on silica. *Langmuir*, **9**, 263–267.

Li, Y.-H. and Gregory, S. (1974) Diffusion of ions in sea water and in deep-sea sediments. *Geochimica et Cosmochimica Acta*, **38**, 703–714.

Li, Z.H. and Bowman, R.S. (1998) Sorption of chromate and PCE by surfactant modified clay minerals. *Environmental Engineering Science*, **15**, 237–245.

Longsworth, L.G. (1960) The mutual diffusion of light and heavy water. *Journal of Chemical Physics*, **64**, 1914–1917.

Lorenzetti, R.L., Shannon, L., Bartelt-Hunt, Burns, S.E., and Smith, J.A. (2005) Hydraulic conductivities and effective diffusion coefficients of geosynthetic clay liners with organobentonite amendments. *Geotextiles and Geomembranes*, **23**, 385–400.

Marry, V., Rotenberg, B., and Turq, P. (2008) Structure and dynamics of water at a clay surface from molecular dynamics simulation. *Physical Chemistry Chemical Physics*, **10**, 4802–4813.

Mazo, M.A., Manevitch, L.I., Gusarova, E.B., Berlin, A.A., Balabaev, N.K., and Rutledge, G.C. (2008) Molecular dynamics simulation of thermomechanical properties of montmorillonite crystal. II. Hydrated montmorillonite crystal. *The Journal of Chemical Physics C*, **112**, 17056–17062.

Meleshyn, A. (2009) Cetylpyridinium aggregates at montmorillonite- and muscovite-water interface: a Monte Carlo study of surface charge effect. *Langmuir*, **25**, 6250–6259.

Meleshyn, A. and Bunnenberg C. (2006) Interlayer expansion and mechanisms of anion sorption of Na-montmorillonite modified by Cetylpyridinium chloride: A Monte Carlo study. *Journal of Physical Chemistry B*, **110**, 2271–2277.

Michot, L.J., Villieras, F., Francois, M., Bihannic I., Pelletier, M., and Cases, J.-M. (2002) Water organisation at solid-aqueous solution interface. *Geoscience*, **334**, 611–631.

Mills, R. (1973) Self-diffusion in normal and heavy water in the range 1–45ºC. *Journal of Physical Chemistry*, **77**, 685–689.

Nakashima, Y. (2003) Diffusion of H_2O in smectite gels: obstruction effects of bound H_2O layer. *Clays and Clay Minerals*, **51**, 9–22.

Nakashima, Y. and Mitsumori, F. (2005) H_2O self-diffusion restricted by clay platelets with immobilized bound H_2O layers: PGSE NMR study of water-rich saponite gels. *Applied Clay Science*, **28**, 209–221.

Oyanedel-Craver, V.A., Fuller, M., and Smith, J.A. (2007) Simultaneous sorption of benzene and heavy metals onto two organoclays. *Journal of Colloid and Interface Science*, **309**, 485–492.

Patel, H.A., Somani, R.S., Bajaj, H.C., and Jasra, R.V. (2007) Preparation and characterization of phosphonium montmorillonite with enhance thermal stability. *Applied Clay Science*, **35**, 194–200.

Revil, A. and Jougnot, D. (2008) Diffusion of ions in unsaturated porous materials. *Journal of Colloid and Interface Science*, **319**, 226–235.

Rytwo, G., Huterer-Harari, R., Dultz, S., and Gonen, Y. (2006) Adsorption of fast green and erythrosine-B to montmorillonite modified with crystal violet. *Journal of Thermal Analysis and Calorimetry*, **84**, 225–231.

Rytwo, G., Kohavi, Y., Botnick, I., and Gonen, Y. (2007) Use of CV- and TPP-montmorillonite for the removal of priority pollutants from water. *Applied Clay Science*, **36**, 182–190.

Schampera, B. and Dultz, S. (2009) Determination of diffusive

transport in HDPy-montmorillonite by H_2O-D_2O exchange using *in situ* ATR-FTIR spectroscopy. *Clay Minerals*, **44**, 249–266.

Shackelford, C.D. and Daniel, E.D. (1991) Diffusion in saturated soil. I: Background. *Journal of Geotechnical Engineering*, **117**, 467–484.

Simonyan, A.V., Behrens, H., and Dultz, S. (2009) Diffusive transport of water in porous feldspars from granitic saprolites: *In situ* experiments using FTIR spectroscopy. *Geochimica et Cosmochimica Acta*, **73**, 7019–7033.

Soule, N.M. and Burns, S.E. (2001) Effect of organic cation structure on behaviour of organobentonites. *Journal of Geotechnical and Geoenvironmental Engineering*, **127**, 363–370.

Tanaka, R. and Hirayama, N. (2008) Crystal structure of benzethonium chloride monohydrate. *Analytical Sciences*, **24**, 163–164,

Van Loon, L.R., Glaus, M.A., and Müller W. (2007) Anion exclusion effects in compacted bentonites: towards a better understanding of anion diffusion. *Applied Geochemistry*, **22**, 2536–2552.

Van Reeuwijk, L.P. (2003) *Procedures for Soil Analysis* (6th edition). ISRIC Technical paper **9**. Wageningen,

Woche, S.K., Goebel, M.-O., Kirkham, M.B., Horton R., van der Ploeg R.R., and Bachmann, J. (2005) Contact angle of soils as affected by depth, texture, and land management. *European Journal of Soil Science*, **56**, 239–251.

Yllera, A., Hernandez, M., Mingarro, A., Quejido, L.A., Sedano, J.M., Soler, J., Samper, J., Molinero, J.M., Barcala, P.L., Martýn, M., Fernandez, P., Wersin, P., Rivas, P., and Hernan, P. (2004) DI-B experiment: planning, design and performance of an in situ diffusion experiment in the Opalinus Clay formation. *Applied Clay Science*, **26**, 181–196.

Zhu, J., Zhu, L., Zhu, R., and Chen, B. (2008) Microstructure of organo-bentonites in water and effect of steric hindrance on the uptake of organic compounds. *Clays and Clay Minerals*, **56**, 144–154.

(*Received 7 October 2009; revised 8 February 2011; Ms. 368; A.E. S. Petit*)